Additive Manufacturing for Advanced Quantum Technologies

F. Wang,[1,*] N. Cooper,[2,*] D. Johnson,[2] B. Hopton,[2] T. M. Fromhold,[2] R. Hague,[1] A. Murray,[1] R. McMullen,[1] L. Turyanska,[1] and L. Hackermüller[2,†]

[1] *Centre for Additive Manufacturing, Faculty of Engineering, University of Nottingham, University Park, Nottingham, NG7 2RD, UK*

[2] *School of Physics and Astronomy, University of Nottingham, University Park, Nottingham, NG7 2RD, UK*

(Dated: March 2025)

The development of quantum technology has opened up exciting opportunities to revolutionize computing and communication, timing and navigation systems, enable non-invasive imaging of the human body, and probe fundamental physics with unprecedented precision. Alongside these advancements has come an increase in experimental complexity and a correspondingly greater dependence on compact, efficient and reliable hardware. The drive to move quantum technologies from laboratory prototypes to portable, real-world instruments has incentivized miniaturization of experimental systems relating to a strong demand for smaller, more robust and less power-hungry quantum hardware and for increasingly specialized and intricate components. Additive manufacturing, already heralded as game-changing for many manufacturing sectors, is especially well-suited to this task owing to the comparatively large amount of design freedom it enables and its ability to produce intricate three-dimensional forms and specialized components. Herein we review work conducted to date on the application of additive manufacturing to quantum technologies, discuss the current state of the art in additive manufacturing in optics, optomechanics, magnetic components and vacuum equipment, and consider pathways for future advancement. We also give an overview of the research and application areas most likely to be impacted by the deployment of additive manufacturing techniques within the quantum technology sector.

INTRODUCTION

Quantum technologies (QT) are expected to have a transformative impact on both research and society, enabling breakthroughs in the study of both fundamental and emergent phenomena as well as underpinning technologies with immediate societal benefits. Some QT devices, such as quantum computers and quantum simulators [1–3], which are expected to drastically expand our ability to understand and simulate a range of complex processes across the natural sciences [4–7], can perform these functions as static devices. Other quantum technologies, such as those associated with quantum cryptography [8, 9], could increase their impact further through portability but are also valuable as fixed installations. Manufacturing requirements for these technologies are currently centered around scalability, stability and rapid prototyping.

However, one of the aspects of QT that is closest to realizing major societal and commercial benefits is quantum sensing. Devices such as atomic clocks [10–13], cold atom gravimeters [14–18], rotation sensors [19–22] and quantum magnetometers [23–25] are presenting opportunities for us to see underground [26–28], navigate without external signals [29, 30] and non-invasively image the structure and function of the human body in real time [31–35]. To be of use, these sensing technologies need to be deployed outside the laboratory, in proximity to the subjects they are supposed to be sensing. In recent years this has created a strong drive towards miniaturization, with a clear need for compact, portable versions of many quantum sensors [36–40]. This need is strengthened further by the recent surge in interest in deploying QT hardware in space [41]; whether for Earth-monitoring applications [42, 43], precisions tests and astronomical observations [44–46] or searches for new physics [47], drastic reductions in size, weight and power consumption (SWAP) are essential for space-based QT. Miniaturization, integration and mass-reduction are therefore key aspects of any manufacturing strategy for quantum sensing technologies.

The last decade has seen dramatic growth of quantum technology sectors and the importance of quantum technologies for global economies – with additive manufacturing (AM) set to enable an impressive improvement in precision and robustness. There are several promising examples of additively manufactured deployable components, with lighter weight, tailored designs allowing fabrication of small numbers of intricate, custom components and embedded functionalities; these are enabled by combining different AM technologies to manufacture a specific part [52] and integrating functional devices with structural architectures and active parts [54]. Here we review recent advancements in manufacturing of QTs enabled by AM, and discuss future perspectives and directions the field is likely to take.

Figure 1 summarizes the benefits AM can offer for various QT devices, both at the level of component fabrication and system assembly. Assembly can be facilitated through the use of AM structural elements, whose main requirements are of shape and physical integrity. AM components include optics, which require accurate shaping, low surface roughness and appropriate transparency and refractive properties, as well as active components

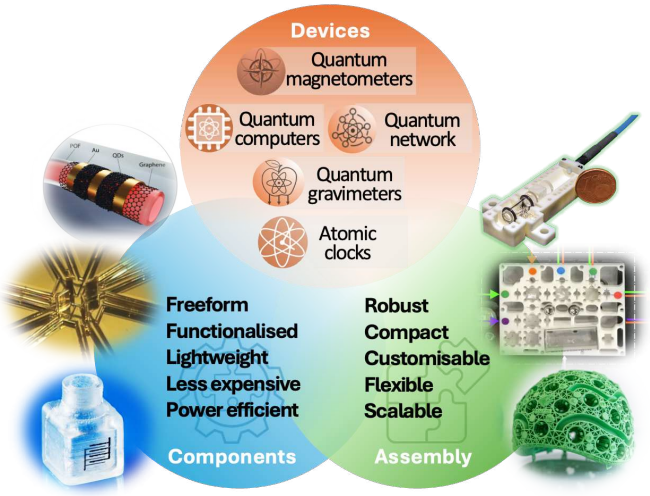

Figure 1. Examples of quantum technology devices and the benefits of AM for component manufacturing and device assembly. The insets are (clockwise from bottom left): a functionalized additively manufactured (AM) vapour cell [48], a printed ion trap for quantum computing [49], an AM photodetector printed directly onto an optical fibre tip [50], a spectroscopic reference system housed in an AM ceramic mount [51], optical apparatus for atom trapping and cooling integrated into an AM polymer framework [52] and an AM helmet for positioning of quantum sensors in a wearable magnetoencephalography system [53].

that integrate conductive pathways and functional electronics within AM materials. Below we give an overview of each of these areas, as well as an assessment of likely future directions and the demonstrated and expected impacts of AM within QT. First, however, we give an overview of the different AM methods used in their production and a brief discussion of design methodology for AM.

ADDITIVE MANUFACTURING METHODS

Several AM techniques have been applied in the production and improvement of quantum devices, as summarized in Figure 2. Extrusion based methods such as fused deposition modeling (FDM) have been used typically in prototyping and manufacturing small structural parts [55]. FDM involves the heating of a thermoplastic filament which is extruded through a nozzle onto a build plate. Similarly, direct writing extrudes high viscosity pastes, polymers and ceramic slurries which are then either dried or cured photochemically. While benefiting from ease of use, cost-effectiveness, and speed, extruded pieces can be prone to structural weakness between printed layers and have a resolution that is limited to nozzle dimensions ($> 50\,\mu$m).

Laser powder bed fusion (LPBF) utilizes a laser or electron beam to fuse together layers of powdered metal, ceramic, or polymeric materials. The print bed is then lowered and fresh powder spread using a recoating lade or roller for the next layer to be fused. The resolution of this technique is controlled by both the laser spot size and the size of the powder particles. The roughness of the surface is able to reach $10\,\mu$m after post-process polishing [56]. The benefits of this technique include the ability to produce miniaturized, lightweight, complex geometries, ideally suited to improving device portability and power density. One drawback of this approach is that substantial heat is dissipated in the build material, which can restrict printing speed and/or cause damaging thermal stresses within the part under construction; designs intended for fabrication via LPBF must account for this to ensure adequate build quality. LPBF has been used to produce a Ni-5Mo-15Fe magnetic shield, a Ti-6Al-4V vacuum flange [57], and an AlSi10Mg coil for magneto-optical atom trapping [58].

Vat polymerization techniques utilize light sources to photochemically cure polymeric resins within a reservoir. Stereolithogray (SLA), digital light processing (DLP), masked stereolithography (mSLA), micro-stereolithography, and emerging technologies such as volumetric additive manufacturing (VAM) [59], and two-photon polymerization (2PP) all fall into this category. These techniques have the advantage of rapidly producing low cost and high-resolution prints, enabling simulated results to be directly implemented into test mounts and expediting design optimization. For example, SLA was employed to rapidly prototype and optimize a monolithic polymer mount for the optical systems required in atom trapping experiments; by directly implementing the functional requirements as efficiently as possible, this device offered significant miniaturization and enhanced stability [52]. Two-photon polymerization processes have improved spatial selectivity, enabling sub-micron resolution, and are well suited for miniaturized, highly-resolved prints [60, 61]. Ceramics and nanoparticles have been added to resins to incorporate additional functionalities to printed pieces, such as conductivity or enhanced mechanical strength [62]. One such resin has been formulated to include 50 wt% fumed silica nanoparticles, and was used to manufacture dense, amorphous glass structures with high optical quality [63]. This material has been used to produce high quality micro-optics and vapor cells capable of ultra-high vacuum levels [48], allowing for Doppler-free spectroscopy and laser frequency stabilization.

Inkjet printing, also known as material jetting, is a well-established technique in conventional graphic printers. Various droplet generation methods are used to produce a stream of, or single, ink droplets that are expelled towards a substrate, allowing for selective patterning without the need for masks. Inkjet printing is capable of printing a wide range of functional materials, with resolution controlled by droplet size and able to reach less

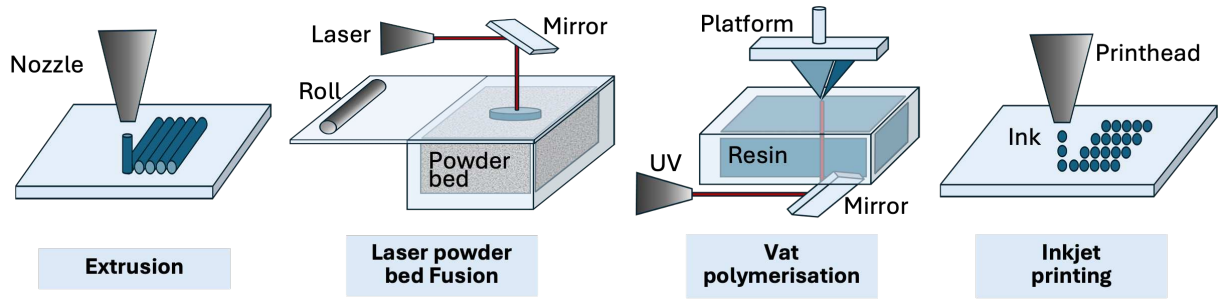

Figure 2. Schematics of different additive manufacturing technologies, which have been applied for quantum technologies.

than 50 μm [64]. Recent research work aimed at expanding the range of compatible inks to include optical, electronic and optoelectronically active materials [65], improving the understanding of material-interface behavior in multi-material prints [66], and investigating the inkjet capability to build 3D-structures [67]. Quantum materials, including quantum dots and perovskite nanoparticles, have been printed using inkjet methods; this technique has created high resolution quantum dot light emitting diode (QLED) devices [68], and a heterogeneous perovskite/graphene photodetector [69].

DESIGN METHODS

A major motivation for developing new systems through additive manufacturing is that the achievable designs are not limited by (traditional) manufacturing methods and can focus on the functional requirements needed for the task—for example following numerical simulation of the device with respect to external stress. In [70], this was done for a 3D-printed vacuum chamber, where the deformation under an external pressure load was analyzed via "Finite Element Analysis" (FEA) based simulation using "MSc Marc 2017.1.0". Based on simulation insights, designs for AM production can be adapted with a high degree of freedom, for example to meet mechanical requirements with minimal addition of material, or to provide additional support along the direction of stress using advanced latticing [71, 72].

AM can also take complex simulations/predictions from theory and directly turn them into an experimentally testable part, matching requirements in areas such as heat dissipation, eddy current response etc. A notable example is the use of AM to create a carefully tailored mass density distribution in order to experimentally test a class of dark matter models, which include domain walls that can be influenced by the local mass density [73].

The high degree of design freedom offered by AM leads to an increasing role for computational design methodologies [74]. These can involve top-down procedural algorithms, for example to map small-scale textures or lattices over complex surfaces [70, 75], as well as standard or machine-learning based strategies for the optimization of one or more build parameters subject to known constraints [76]. The application of such methods within QT will enable specific experimental needs to be met with maximum efficiency.

STRUCTURAL ELEMENTS

Structural elements are typically used for assembly of components and their protection from mechanical damage. They are essential for quantum technologies, e.g. to deliver stable and reliable optical systems or correctly position coils and magnetic shields with complex geometries.

All structural components benefited from mass reduction opportunities [77–79], including several in QT applications [57, 70], achieved through "structural optimization": the process of shaping a component so as to meet mechanical specifications with a minimum amount of total material, usually with the aid of computational design tools [80, 81]. This process often results in complex, organic-looking forms and/or intricate, small-scale patterning that would be highly impractical with conventional manufacturing; see, for example, the AM vacuum chamber shown in Figure 4(a). Usually, structural optimization relies on "latticing" - the replacement of a solid volume of material with numerous, interconnected struts whose exact shape and density can be varied to meet specific requirements [71, 72].

The role of structural components was expanded to, facilitate rapid heat dissipation from key areas [82, 83] and damping or isolating mechanical vibrations to improve stability [84–86]. These capabilities have proved transformative for other sectors, and their wider deployment within QT is likely to have substantial impact on the sector. Below, we consider two areas of particular relevance to QT: optomechanics and vacuum equipment.

Optomechanics and component positioning

Many QT hardware components require accurate positioning, often within complex, multi-component systems. AM allows rapid and cost-effective production of intricate, bespoke mounting systems that accelerate prototyping and research. For example, the success of recent work on brain pattern imaging with atomic magnetometers has depended in part on a lightweight AM helmet [31, 53] for appropriate positioning of the magnetometers on a mobile subject (see Figure 3(c)). The construction allows a highly robust and wearable OPM system with a total weight (including sensors) of 1,7 kg. The rigid helmet was additively manufactured from PA12 (a nylon polymer) using an EOS P100 Formiga Laser Sintering machine. AM enables 133 cylindrical sensor mounts, eliminating motion of any sensor relative to all other sensors, while ensuring air circulation through a stable matrix-based gyroid triply periodic minimal surface lattice between the sensors. The relative locations and orientations of the sensor mounts are known to a high level of accuracy, because a complete digital representation of the helmet exists, and the tolerance of the 3D printing process is approximately 300 μm. Another example is the magnetometer array described in [55] and shown in Figure 3(e), in which an AM mount ensures correct relative positioning of all system components.

Of particular relevance to QT is the positioning of optical components, such as mirrors and lenses, within the optical subsystems of QT devices. Here, not only the positions but also the *orientations* of all components must be set and maintained with high precision—orientation control in such optical systems is often needed at the sub-milliradian level. AM shows particular promise in this area because the miniaturization enabled by AM reduces the stringency of orientational alignment requirements; compact AM versions of optical systems have been found to demonstrate superior stability in consequence [51, 52, 87].

The following formula for the approximate position deviation of a laser beam after passing through an optical system is given in [52]:

$$\Delta r = \left[\Sigma_i (2\Delta\phi L_i)^2\right]^{1/2}, \tag{1}$$

where Δr is the position uncertainty of the beam's center in some plane of interest, each reflective optic in the beam path is assumed to have independent alignment uncertainty $\Delta\phi$ and L_i is the path length from the optic i to the plane of interest. Where the scale of $\Delta\phi$ is independent of the size of the system this indicates a linear scaling of beam position uncertainty with optical path length; in reality the relative alignment deviations of components are likely to be greater for larger systems, due to the lower degree of curvature required in a mounting structure to achieve the same angular deviation when the spatial separation is greater. This formula thus illustrates the extreme importance of miniaturization in creating stable and robust optical apparatus, underpinning the success not only of [52] but also of subsequent developments such as [51], and highlighting the importance of miniaturization for achieving *stable* QT devices as well as portable ones.

With this in mind, drastic miniaturization of such optical systems has been accomplished by embedding the optics within custom-built polymer [52, 87] or ceramic frames [51], where the suitability of AM for economic production of small batches of intricate components has facilitated both miniaturization and stability by eliminating the need for adjustable components in these mounting systems. In [87], an atomic spectroscopy apparatus with a total volume of < 0.1 l and a mass of 120 grams is demonstrated (see Figure 3(d)), with a point of particular interest being that it is produced from polylactic acid (PLA) via FDM. Based on AM design and fabrication this device achieves remarkable stability. PLA and FDM are a common and economic AM material and method, and the relevant material properties of PLA, such as elastic modulus and coefficient of thermal expansion, are not particularly favorable for device stability. Despite this, the device demonstrated in [87] achieves far greater stability and robustness against environmental influence than standard lab systems; it is able to keep a laser frequency-stabilized to an atomic transition despite being subjected to temperature variations between 7 and 35 °C and significant vibrational disturbances in a frequency range from 0 to 2 kHz. This illustrates how miniaturization and careful design, exploiting the freedom provided by AM, can overcome the limitations of build materials and deliver high overall performance with both low SWAP and low cost.

Subsequent work has applied the same approach with more advanced materials and methods, leading to further performance enhancements. For example, in [51] a miniaturized spectroscopic frequency reference device is demonstrated with a total volume of 5.6 ml and a mass of 15 grams (Figure 3(f)). Laser frequency stabilization is implemented using the spectroscopic signal from this device and enables frequency instabilities as low as 1.5 kHz over 100 s, and < 40 kHz over 10^4 s; stability is in part aided by the very short total optical path length of 53 mm. The materials and methods demonstrated in [51] were subsequently adapted to demonstrate a highly-compact optical dipole trap for ^{87}Rb atoms, a critical subsystem of many quantum sensing technologies [88].

Vacuum components

While vacuum apparatus is in essence a structural element, its use in high-vacuum applications places more stringent requirements on the methods and materials in-

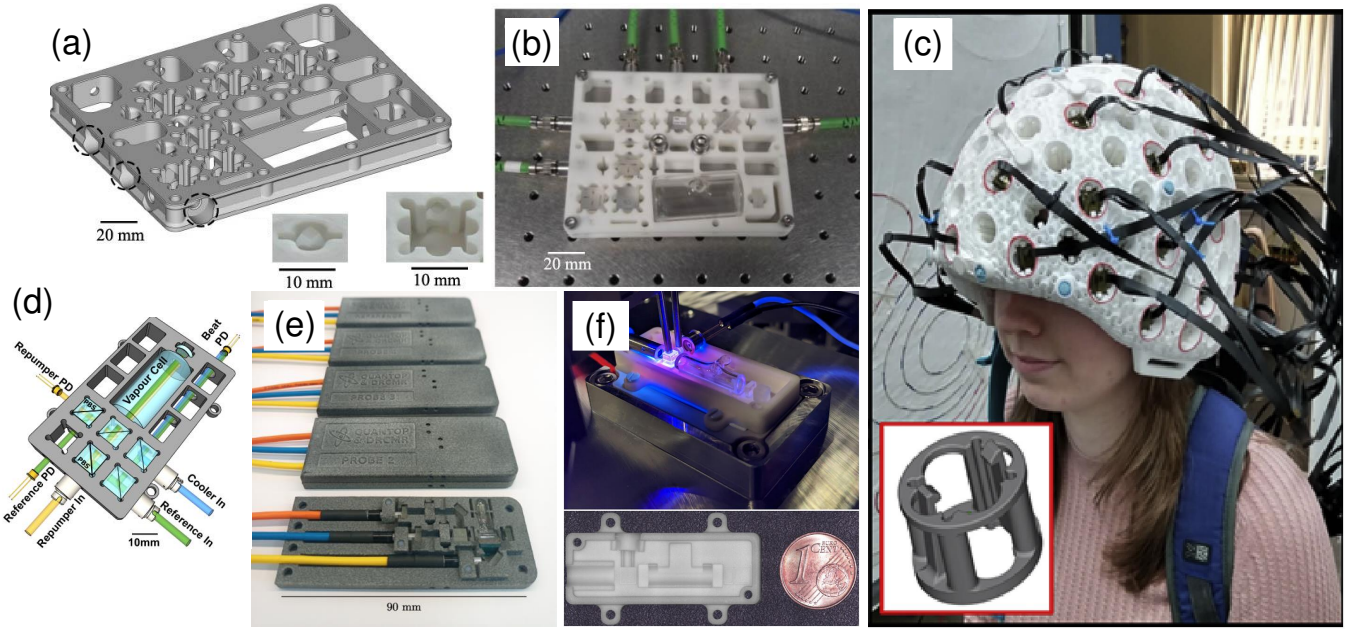

Figure 3. (a) Design of an AM optical mounting framework for compact magneto-optical trapping apparatus [52], including frequency stabilization for three wavelengths and power distribution into three optical fibers. (b) The final system printed in reinforced resin [52] contains no movable elements apart from rotatable waveplates that are glued in place after alignment. (c) A 3D-printed helmet for exact positioning of optically-pumped magnetometer (OPM) devices [53]. (d) Compact spectroscopy and frequency stabilization system for three frequencies printed in polylactic acid via FDM [87]. (e) Magnetometer array for high precision spectroscopy [55] following the approach of [52]. (f) Miniaturized spectroscopic reference apparatus that exploits a ceramic AM mounting structure, as described in [51].

volved; vacuum apparatus must be leak-tight, able to make sealed connections to other vacuum components, have sufficient mechanical strength to survive robust assembly and atmospheric pressure, and be free from both trapped gas pockets and materials that outgas excessively.

The high and ultra-high vacuum (UHV) regimes are most relevant to QT, as maintaining quantum coherence requires minimal interactions with unwanted gas particles. AM was not initially considered appropriate for UHV due to its characteristic rough surfaces and porosity, and early attempts to apply AM to high-vacuum apparatus achieved only modest performance [89]. The first widely-publicized examples of AM components operating in the UHV regime occurred in 2018 with an AM-flange [57] and 3D-printed in-vacuum coils [58], as seen in Figure 4(b). These were subsequently followed by the demonstration of a full vacuum chamber produced via powder-bed fusion [70]. These demonstrations showed that porosity could be reduced to acceptable levels through appropriate build procedures and post-processing heat treatments, while surface roughness appeared not to be as destructive to vacuum performance as previously feared.

A number of different materials and methods have been explored for AM vacuum components. While [58, 70] used AlSi10Mg produced via laser powder-bed fusion, high-vacuum components have also been additively manufactured in Titanium [57, 91] and stainless steel [89, 92] via the same method and in glass [48] and aluminium oxide [51] using vat polymerization. Meanwhile, Ratkus et al. have obtained promising initial results for vacuum compatibility from test samples of AM copper, produced using LPBF [93]. Though techniques involving a binding agent, such as binder jet printing [94], have not yet been as successfully applied to metal AM for UHV, the above demonstrations of ceramic components fabricated using ceramic-doped polymers indicate that the use of a removable binding agent does not preclude a method for UHV applications.

Recently, the suitability of printed plastics for HV and UHV has been explored, with a number of materials fabricated via FDM and mSLA found to be suitable for deployment in HV and even UHV conditions [95, 96]. In particular, the proprietary material Tullomer was found to exhibit desorption rates as low as $5\times10^{-11}\,\mathrm{mbar\,l\,cm^{-2}s^{-1}}$ [95], with vessels containing printed test-samples reaching pressures below $10^{-9}\,\mathrm{mbar}$.

The application of thin, UHV-compatible coatings to more traditional AM materials has also been found to be effective in improving vacuum performance [97]. Evidence was found in [70] to suggest that the material outgassing rate was being reduced by a protective surface layer, indicating that this approach is applicable across

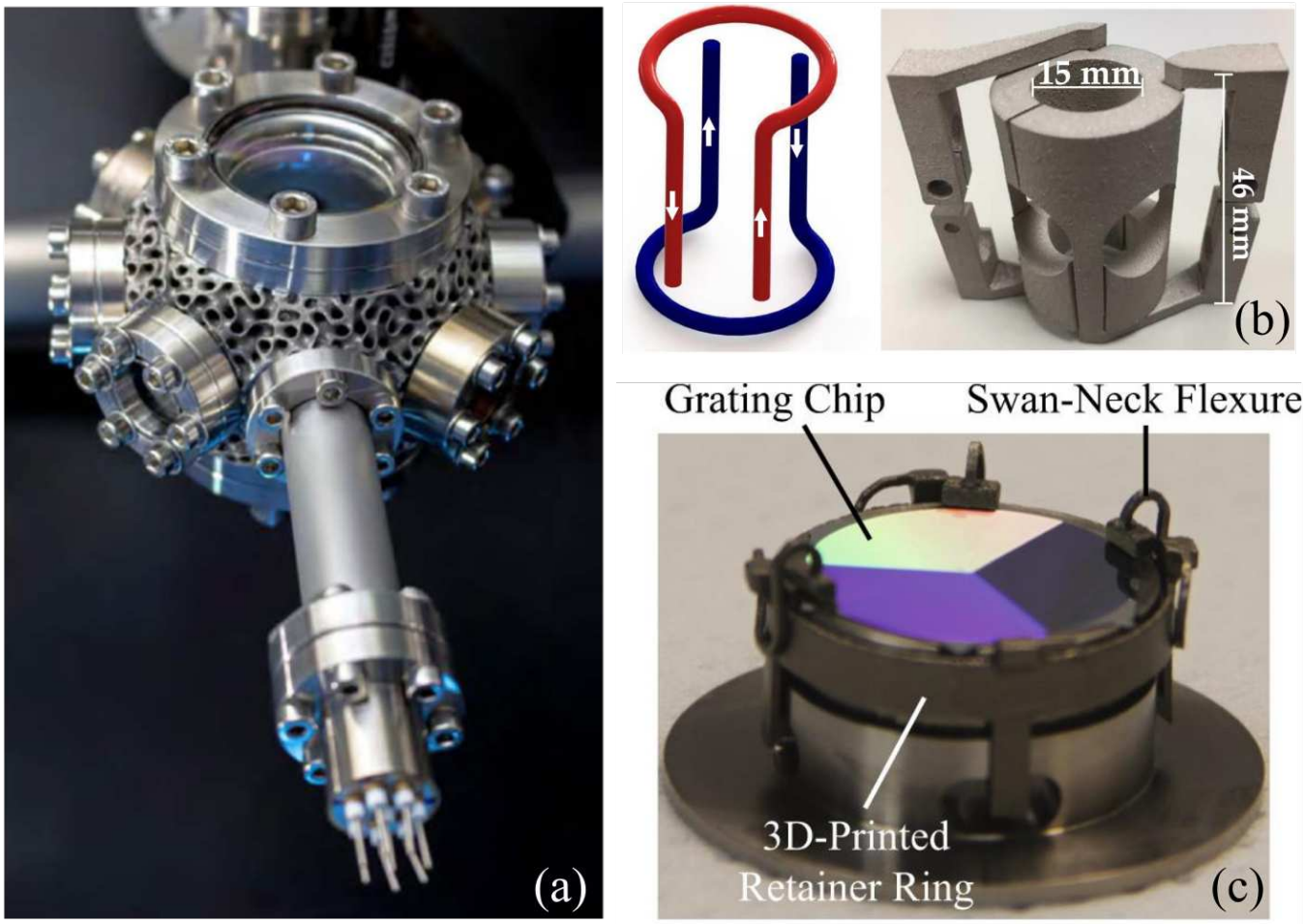

Figure 4. Additively manufactured components for UHV systems. (a) AM UHV chamber demonstrated in [70]. Structural optimization, taking the form of a gyroid lattice, is visible on the chamber exterior and enables considerable mass reduction. (b) AM coils for a magneto-optical trap described in [58] and sketch illustrating current flow during operation. (c) An AM grating mount for a single-beam magneto-optical trap [90]; AM enables a bespoke swan-neck flexure mount and avoids the use of epoxies.

different materials and AM methods.

The potential advantages of AM for vacuum components are numerous, and perhaps the best way to review them is to examine representative examples of each case. There is, naturally, significant overlap with the benefits of AM for other structural components. Light-weighting has been demonstrated in [70], where a structure feasible only via AM enabled a mass reduction of approximately one third (the chamber in fact weighed around 70% less than industry-standard equivalents, but not all of this advantage stemmed from AM-specific developments). Meanwhile, [58] illustrated the benefits of rapid prototyping and the ease of fabricating custom components to meet specific requirements, using AM to produce a set of coils for magneto-optical trapping with unusually low power consumption and switching time. While conventional fabrication of this coil structure would have been possible, AM enabled rapid production and testing of an unusual structure specific to the needs of an individual experiment. The AM AlSi10Mg that comprised these coils was produced using laser powder bed fusion and yielded a cold resistivity of 5×10^{-8} Ωm, or a conductivity that is 70% of the bulk material.

In [90] a grating chip used for magneto-optical atom trapping was held in place with an additively manufactured retainer that has four swan-neck flexure mounts using Ti-alloy (ASTM Ti-6Al-4V)—see Figure 4(c). The flexure mounts provided excellent optical access to the surface of the grating chip and avoided the use of epoxies.

Beyond these demonstrated examples, additive manufacturing of UHV components promises a range of further benefits for QT. One is part consolidation. Most current UHV systems are assembled from modular components to enable the construction of bespoke systems from industry standard parts that can be efficiently man-

ufactured using conventional techniques. Because of the need to maintain a vacuum seal, the connections between these modular components are bulky and laborious to assemble; eliminating them through part consolidation facilitates rapid prototyping and leads to considerable miniaturization and mass reduction. Consolidation also aids reliability by reducing the number of potential leak locations. AM allows efficient production of customized systems, removing the need for modular components and thus enabling part consolidation. Other potential areas of benefit include selectively screening key experimental regions from known outgassing sources, finely controlling gas flow and channel conductance and tailoring the eddy current response of conductive structures to changes in magnetic field. Ongoing work by the authors is also showing that AM-enabled surface patterning can improve the effectiveness of passive pumping systems based on non-evaporable getters [98]. All of these have clear usage cases within QT and stand to be enabled or facilitated by the advancement of AM for UHV applications.

TRANSPARENT ELEMENTS AND OPTICS

Transparent optical and photonic components are essential in quantum technology applications for beam shaping, collimation, focusing, transmission and imaging. With its expanding material libraries encompassing polymers, silica, and low dimensional materials, AM offers a flexible approach for producing complex micro-optics. These include lenses, waveguides and coupling interfaces for integration, with applications in quantum sensing, information processing and more. For instance, micro-lens arrays of different sizes and geometries have been fabricated using both inkjet printing and SLA. Inkjet printing shows great potential for fabricating polymer convex or hemispherical refractive micro-lens arrays with diameters from 100 μm to several mm, offering high flexibility, minimal processing complexity and low production cost. Xie et al. have fabricated an array of 9×9 polymeric micro-lenses with a diameter of 333.3 μm, a pitch of 354.04 μm, a sag height of 94.13 μm and surface roughness of 0.243 nm using UV curable polymers [99]. The pitch and the geometry of the micro-lens array are uniform (Figure 5(a)). For micro-lenses of $< 50\,\mu$m diameter, digital light processing methods are advantageous. A 2×2 micro-spherical lens array with diameter of 15 μm and a micro Fresnel lens with diameter of 17 μm have been been fabricated by Guo et al. using two-photon polymerization, as shown in Figure 5(b) [100]. Here a SCR500 acrylate resin was used with a transparency in the visible range of 85-90%.

Similarly, internal reflection solid immersion lenses can be fabricated on top of single InAs quantum dots [101, 105] and have increased the collection efficiency of the output photons by up to 9 times when aligned with gold markers (Figure 5(c)). The single-photon character of the source is preserved after device fabrication, reaching a degree of second-order coherence value of approximately 0.19 under pulsed optical excitation. The printed lens device can be further joined with an optical fiber and permanently fixed to the fiber [105].

Limitations for transparent polymers and oligomers relating to chemical compatibility, vacuum compatibility, temperature tolerance, material leeching [106] and air-permeability pose challenges for QT applications. Glass is often a more desirable material due to its chemical inertness, high transparency across a wide spectral range and physical tolerances. AM of glass typically involves a fumed silica nano-powder resin which is then thermally processed after printing to remove unwanted compounds and sinter the aggregated powder into transparent glass. Kotz et al. [63] have demonstrated micro-optical diffractive elements and glass micro-lens arrays by micro-stereolithography, with a surface roughness of about 2 nm (Figure 5(d)). The structure exhibits 90% transparency for wavelengths from UV to near-infrared.

Functional materials for active QT-components can be integrated into micro-optical structures. For example, Nitrogen vacancy (NV) defects in diamond have been demonstrated as quantum sensors [107, 108], where their properties are affected by environmental factors such as magnetic field, pressure or temperature. Nanodiamonds have been incorporated into additively manufactured components [109], but nanodiamond loading has to be well-controlled to prevent structural deformation due to light scattering during the printing process. For 0.002 wt% loading, NV-nanodiamond clusters can clearly be seen in AM structures fabricated via two-photon polymerization (Figure 5(e) [102].

Apart from micro-lenses, waveguides can also be fully fabricated by AM and might be used in the future for quantum sensing [110] or quantum computing [111, 112]. Hybrid organic–inorganic optical waveguides have been demonstrated in straight, curved, and out-of-plane configurations via direct-write assembly of photo-curable liquid core-–viscoelastic fugitive shell inks by Lorang et al., as shown in Figure 5(f) [103]. The printed waveguides exhibit nearly cylindrical morphology and low optical loss throughout the visible spectrum. For nanoscale photonic interconnections, Pyo et al. reported a meniscus-guided 3D printing method that allows direct, non-destructive integration of nanowire waveguides, as shown in Figure 5(g) [104]. No substrate leakage and excellent stretchable operations were observed for functional photonic components of multiplexers and splitters.

Micro-lenses have also been directly fabricated on the end facet of single-mode optical fiber to collimate a Gaussian beam emerging from the fiber. Spherical lenses with different radii of curvatures and thicknesses have been produced by Gissibl et al. [113], the schematic shape and the resulting beam waist has been studied, showing that

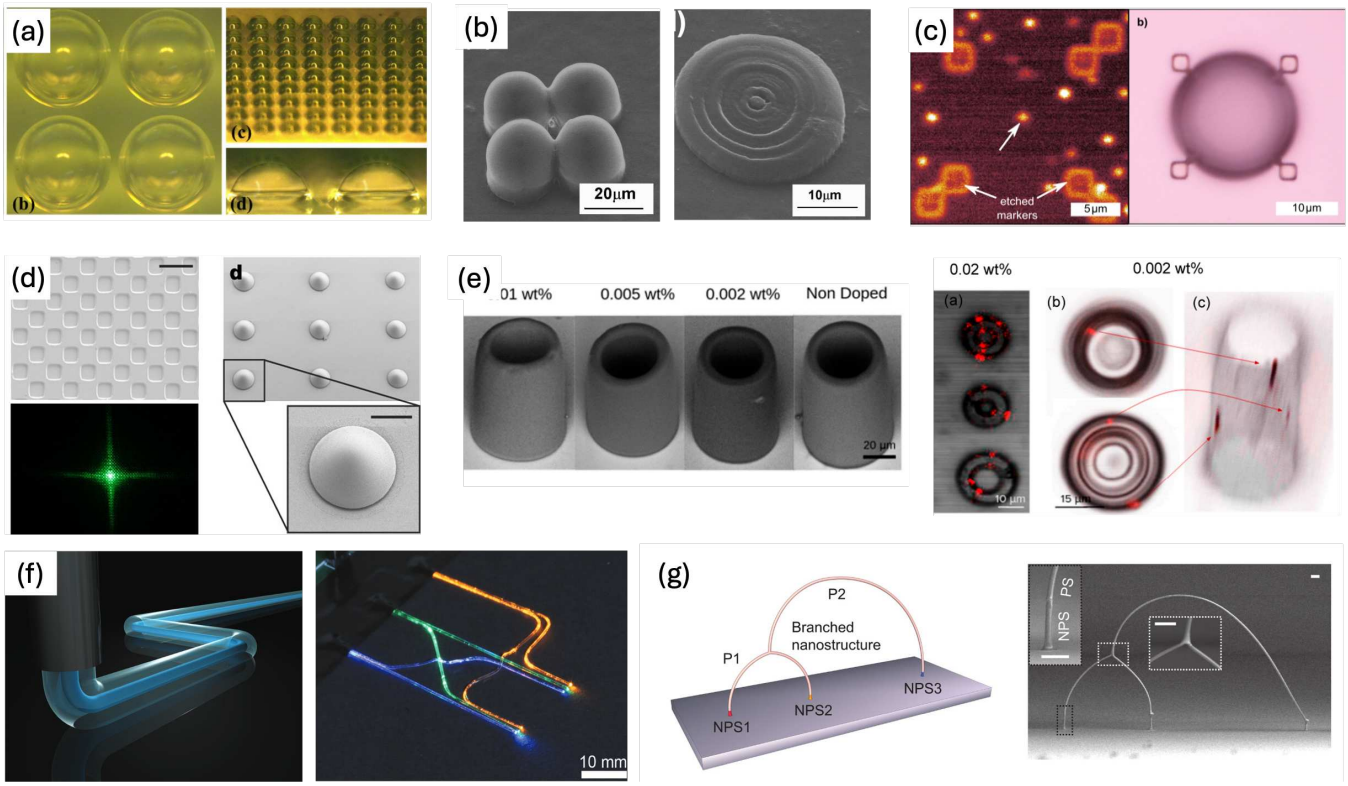

Figure 5. Examples of transparent optical components by AM for quantum technologies. (a) Micro-lens array of average diameter 333.28 μm by inkjet printing [99]. (b) Spherical micro-lenses (left) and micro Fresnel lens fabricated by two-photon polymerization [100]. (c) Photoluminescence intensity map (left) and the optical microscope image (right) of solid immersion lens printed on the single quantum dot for light coupling [101]. (d) Glass micro-optical diffractive structure with the optical projection pattern (left) and microlenses fabricated using micro-stereolithography. (scale bar: 100 μm). Reprinted with permission from [63]. (e) Left: scanning electron microscope image of cylindrical microstructues fabricated using two-photon polymerization, doped with different proportions of nanodiamonds. Right: confocal scanning image and 3D rendering of structures doped with 0.02 wt% nanodiamond showing fluorescent spots artificially coloured [102]. (f) Left: schematic image of a direct-write assembly of photocurable liquid core-fugitive printed polymeric optical waveguides. Right: an optical waveguide network composed of six waveguides coupled with three LEDs that distributed colored light with minimal crosstalk. Reprinted with permission from [103]. (g) Schematic diagram and scanning electron microscopy images illustrating a freestanding branched structure integrated on three different nanophotonic sources by meniscus-guided 3D printing. The white scale bars in the right-hand panel are 2 μm in length. Reprinted with permission from [104].

the collimation improves with increasing lens thickness (Figure 6(a)). Additionally, the measured intensity distribution was used to infer the real surface profile and thus, via an iterative optimization algorithm, to improve the fabrication process. Furthermore, micro-lenses printed onto the tip of standard optical fibers have enabled a new trapping concept for ultracold atoms in optical tweezers [114]. The unique properties of these lenses make them suitable for both trapping of small numbers of atoms and capturing their fluorescence with high efficiency. In an exploratory experiment by Ruchka et al. (Figure 6(b)) [114], the vacuum compatibility and robustness of these structures were demonstrated, and a magneto-optical trap for ultracold atoms was successfully formed approximately 125 μm from the fibre tip.

ACTIVE COMPONENTS

The scope of AM for quantum technologies can be greatly expanded by incorporating functional materials for active components into the printed structure. Recently, an atomic vapor cell that was printed using vat polymerization [48] has been demonstrated. This cell, measuring 7 mm per side, was pumped to 2×10^{-9} mbar, maintaining this pressure with no noticeable leaks, before being filled with Rb vapor (Figure 7(a)). A laser was passed through the cell and the resulting spectroscopy was used to frequency stabilize a laser to the $F = 2 \rightarrow F' = 3$ transition of ^{85}Rb. The Allan deviation of the error signal was measured for a range of time scales, yielding a frequency instability of $\Delta F/F = 2 \times 10^{-10}$ for integration times of 1 s. This performance was found to be approximately the same as the frequency stabil-

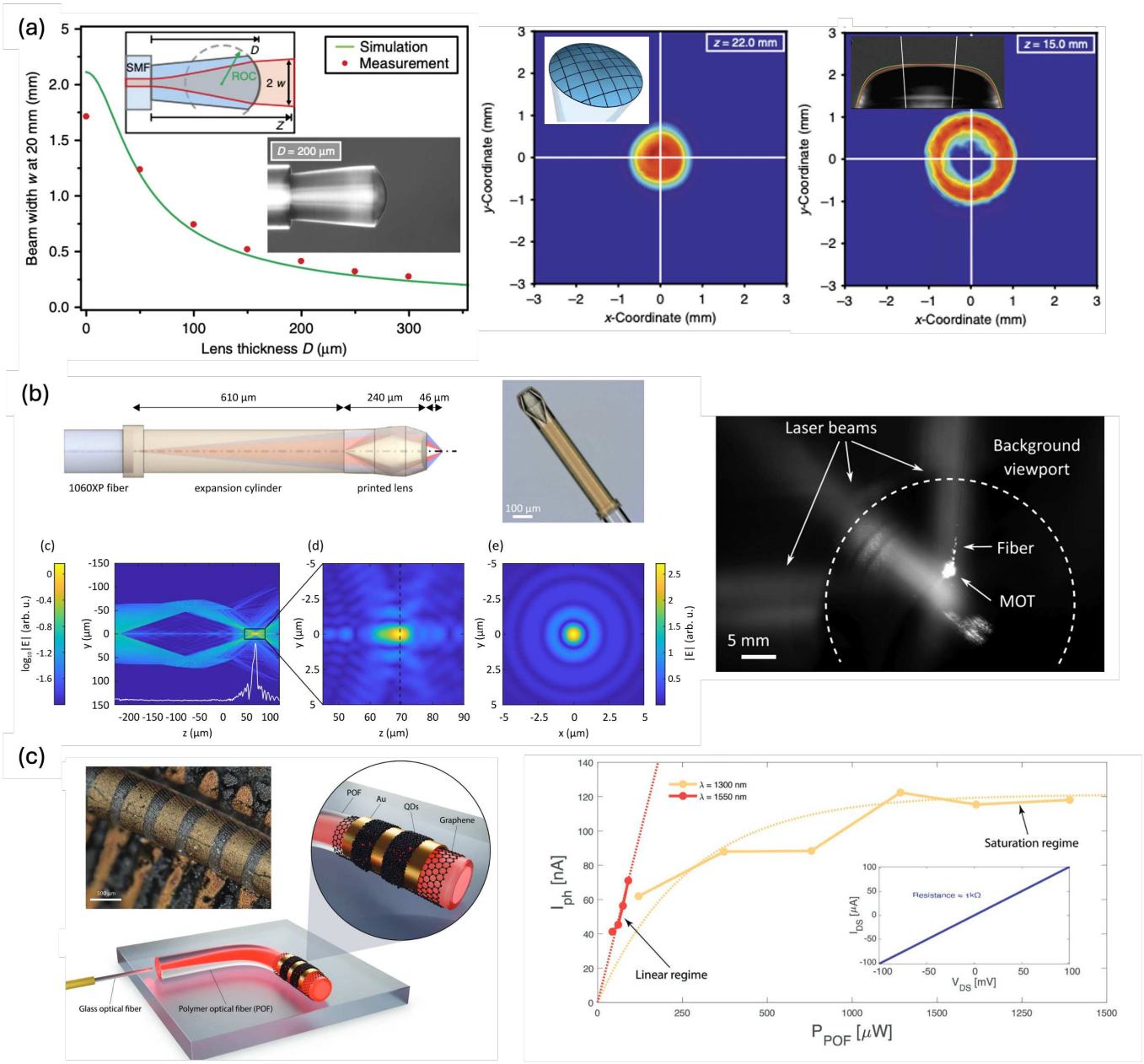

Figure 6. Printing components on optical fibers for quantum technology applications. (a) Left: design and optical microscope images of spherical lenses fabricated by direct laser writing with thicknesses ranging from 0 to 300 mm and the corresponding beam width. Center: donut shaping free-form lens and the measured light distribution. Right: top-hat light shaping free-form lens and the measured light distribution [113]. (b) Left: a total internal reflection lens printed at the tip of a fiber and the wave propagation method simulated electric field with a zoom into the focal region and the radial cross-section at the focal spot. Right: creation of a MOT 125 μm from the fiber tip with the TIR lens when positioned in the center of a UHV chamber [114]. (c) Left: schematic and optical microscope image of the hybrid-PbS quantum dot phototransistor printed on polymer optical fiber. Right: the photocurrent of the phototransistor under different light power for 1300 and 1550 nm wavelengths[50].

ity achieved with a laser locked to a Thorlabs borosilicate cell, when normalized for the difference in optical path length. Integrated multi-material components, such as inkjet printed graphene and silver electrodes, are also demonstrated in [48]; these and similar elements are promising for applications such as photon detection, localized heating and active magnetic shielding.

Another key active QT component recently demonstrated is a 3D-printed micro ion trap for quantum information processing by Xu et al. [49]. The trap is fabricated by first creating 3D polymer structures using two-photon polymerization and then coating the poly-

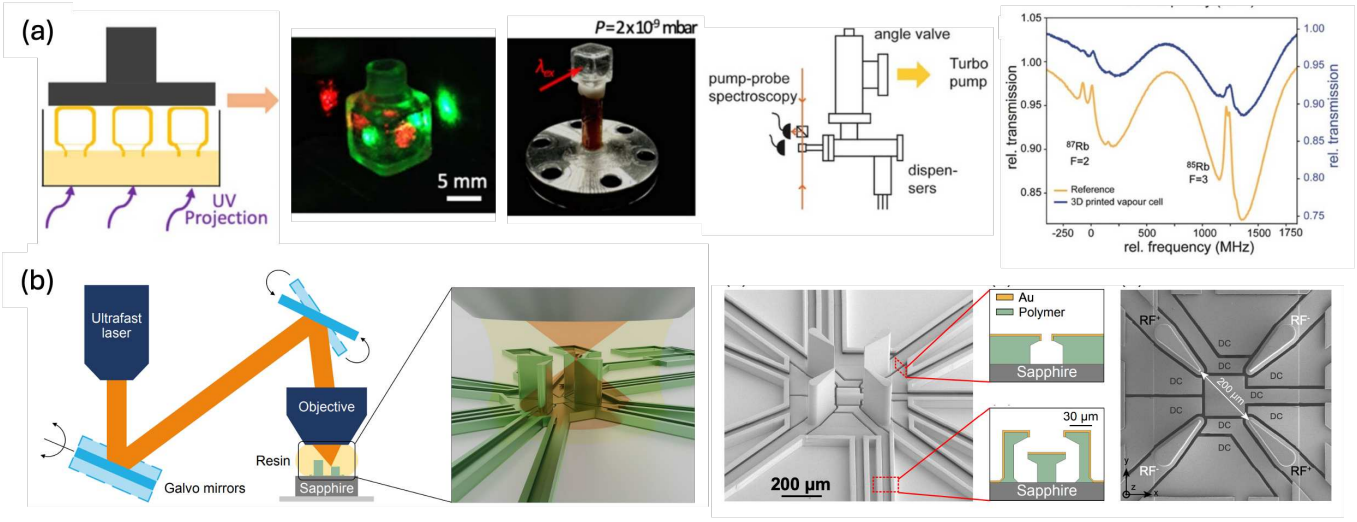

Figure 7. Examples of active components made by AM for quantum technology applications. (a) An glass vapor cell fabricated using vat polymerization, with cuboid shape and two clear optical axes. The cell is mounted to a standard UHV system to demonstrate Rb hyperfine spectroscopy [48]. (b) Illustration and scanning electron microscope images of a 3D-printed vertical linear Paul trap, with coated gold electrodes for RF and DC voltages to achieve ion-trap quantum computing [49].

mer with a 1 µm-thick gold layer using electron-beam evaporation (Figure 7(b)). The trap consists of four RF electrode pillars on a sapphire substrate with a total height of 300 μm. Nine planar DC electrodes are placed on the substrate surface for tuning the potential in a 600 μm × 600 μm square. Single calcium ions have been confined in the 3D printed trap with radial frequencies ranging from 2 MHz to 24 MHz under room temperature, enabling high-fidelity coherent operations on a Ca^+ optical qubit after only Doppler cooling. The design freedom of AM offers an opportunity to scale this initial demonstration into multi-dimensional ion trap arrays with optimized performance and expanded functionality. Underpinned by integrated photonic circuits based upon AM waveguides, this architecture may have significant potential for scalable quantum computing.

CONCLUSION AND OUTLOOK

AM has a demonstrated ability to substantially advance quantum technologies by enabling the fabrication of intricate, highly customized and scalable components. This review has highlighted the diverse applications of AM in quantum technology devices demonstrated to date, including structural components for assembly and high-vacuum apparatus, optical and photonic components, and functionalized active components. Quantum technologies can benefit in multiple ways from AM, including via reductions in SWAP, improved stability, and the enabling of integrated, multi-material structures not possible through conventional manufacturing, such as those demonstrated in [48, 49]. Integration of the advantages of AM with the needs of QTs could bring transformative changes in sectors from healthcare and navigation to computing and communication. Particularly important are developments in the quantum sensing area, where AM of components for high vacuum applications was demonstrated with metal, glass and even polymers to produce parts with a high degree of design freedom, tailored to specific applications [54, 70].

Quantum sensing is a fast growing area, which is currently largely limited to high value applications due to complexities in device manufacturing, operational environmental requirements and the advanced operator skill set needed; a manufacturing approach that focuses on design freedom and the efficient realization of complex parts, rather than on large production volumes, is urgently needed to enable these transformative applications. AM will be of increasing importance to the deployment of quantum sensors in the near future. Current research addresses open questions on the long-term stability of components, the fabrication precision of AM for certain techniques and material compatibility [115, 116]. In this fast-evolving field we are witnessing the development of novel printable materials, deposition strategies and multi-material AM [65]. Furthermore, hybrid approaches that combine AM with traditional microfabrication techniques can enhance the performance and reliability of quantum components [117, 118]. Looking ahead, AM has the potential to provide an ideal manufacturing solution for emerging quantum technologies and enable the widespread use of quantum systems outside the laboratory, notably in key environments such as in space, on vehicles or underground. Combining the benefits of optimized design with on-site, on-demand manufacturing

of compact and packaged field-deployable devices, AM will help to accelerate the development and commercialization of quantum technologies. However, the development of AM supported quantum technologies has only just begun, and key foundational advancement might await in the near future, in the development of the interface between quantum science and technology and the materials and processes of additive manufacturing: for example via research into AM of active quantum materials, complete QT-AM sensors or sensor arrays or AM supported quantum computers or optimization of AM materials and processes with respect to the sensitivity and long-term precision and stability of AM fabricated quantum sensors. Continued interdisciplinary research is therefore critical in overcoming existing technical barriers and supporting the realization of the transformative promise held by quantum technologies.

Acknowledgments

We acknowledge supported by the grant 62420 from the John Templeton Foundation, the IUK project No.133086, EPSRC grants EP/T001046/1, EP/R024111/1, EP/M013294/1, EP/Y005139/1 and EP/Z533166/1.

* The first two authors contributed equally to this work
† Corresponding author:
lucia.hackermuller@nottingham.ac.uk

[1] A. Steane, Quantum computing, Reports on Progress in Physics **61**, 117 (1998).
[2] T. D. Ladd, F. Jelezko, R. Laflamme, Y. Nakamura, C. Monroe, and J. L. O'Brien, Quantum computers, Nature **464**, 45 (2010).
[3] S. Lloyd, Universal quantum simulators, Science **273**, 1073 (1996).
[4] E. F. Dumitrescu, A. J. McCaskey, G. Hagen, G. R. Jansen, T. D. Morris, T. Papenbrock, R. C. Pooser, D. J. Dean, and P. Lougovski, Cloud quantum computing of an atomic nucleus, Phys. Rev. Lett. **120**, 210501 (2018).
[5] A. Kandala, A. Mezzacapo, K. Temme, M. Takita, M. Brink, J. M. Chow, and J. M. Gambetta, Hardware-efficient variational quantum eigensolver for small molecules and quantum magnets, Nature **549**, 242 (2017).
[6] B. P. Lanyon, J. D. Whitfield, G. G. Gillett, M. E. Goggin, M. P. Almeida, I. Kassal, J. D. Biamonte, M. Mohseni, B. J. Powell, M. Barbieri, A. Aspuru-Guzik, and A. G. White, Towards quantum chemistry on a quantum computer, Nature Chemistry **2**, 106 (2010).
[7] A. Robert, P. K. Barkoutsos, S. Woerner, and I. Tavernelli, Resource-efficient quantum algorithm for protein folding, npj Quantum Information **7**, 38 (2021).
[8] N. Gisin, G. Ribordy, W. Tittel, and H. Zbinden, Quantum cryptography, Rev. Mod. Phys. **74**, 145 (2002).
[9] S. Pirandola, U. L. Andersen, L. Banchi, M. Berta, D. Bunandar, R. Colbeck, D. Englund, T. Gehring, C. Lupo, C. Ottaviani, J. L. Pereira, M. Razavi, J. S. Shaari, M. Tomamichel, V. C. Usenko, G. Vallone, P. Villoresi, and P. Wallden, Advances in quantum cryptography, Adv. Opt. Photon. **12**, 1012 (2020).
[10] S. Bize, P. Laurent, M. Abgrall, H. Marion, I. Maksimovic, L. Cacciapuoti, J. Grünert, C. Vian, F. P. Dos Santos, P. Rosenbusch, *et al.*, Cold atom clocks and applications, J. Phys. B **38**, S449 (2005).
[11] A. D. Ludlow, M. M. Boyd, J. Ye, E. Peik, and P. O. Schmidt, Optical atomic clocks, Rev. Mod. Phys. **87**, 637 (2015).
[12] J. Grotti, I. Nosske, S. Koller, S. Herbers, H. Denker, L. Timmen, G. Vishnyakova, G. Grosche, T. Waterholter, A. Kuhl, S. Koke, E. Benkler, M. Giunta, L. Maisenbacher, A. Matveev, S. Dörscher, R. Schwarz, A. Al-Masoudi, T. Hänsch, T. Udem, R. Holzwarth, and C. Lisdat, Long-distance chronometric leveling with a portable optical clock, Phys. Rev. Appl. **21**, L061001 (2024).
[13] W. Loh, D. Reens, D. Kharas, A. Sumant, C. Belanger, R. T. Maxson, A. Medeiros, W. Setzer, D. Gray, K. DeBry, C. D. Bruzewicz, J. Plant, J. Liddell, G. N. West, S. Doshi, M. Roychowdhury, M. E. Kim, D. Braje, P. W. Juodawlkis, J. Chiaverini, and R. McConnell, Optical atomic clock interrogation using an integrated spiral cavity laser, Nature Photonics 10.1038/s41566-024-01588-8 (2025).
[14] M. Kasevich and S. Chu, Atomic interferometry using stimulated raman transitions, Phys. Rev. Lett. **67**, 181 (1991).
[15] A. Peters, K. Y. Chung, and S. Chu, Measurement of gravitational acceleration by dropping atoms, Nature **400**, 849 (1999).
[16] C. Ruan, W. Zhuang, J. Yao, Y. Zhao, Z. Ma, C. Yi, Q. Tian, S. Wu, F. Fang, and Y. Wen, A transportable atomic gravimeter with constraint-structured active vibration isolation, Sensors **24**, 2395 (2024).
[17] C. Cassens, B. Meyer-Hoppe, E. Rasel, and C. Klempt, Entanglement-enhanced atomic gravimeter, Phys. Rev. X **15**, 011029 (2025).
[18] E. R. Elliott, D. C. Aveline, N. P. Bigelow, P. Boegel, S. Botsi, E. Charron, J. P. D'Incao, P. Engels, T. Estrampes, N. Gaaloul, J. R. Kellogg, J. M. Kohel, E. Norman, N. Lundblad, M. Meister, M. E. Mossman, G. Mueller, H. Mueller, K. Oudrhiri, L. E. Phillips, A. Pichery, E. M. Rasel, C. A. Sackett, M. Sbroscia, W. P. Schleich, R. J. Thompson, and J. R. Williams, Quantum gas mixtures and dual-species atom interferometry in space, Nature **623**, 502–508 (2023).
[19] T. L. Gustavson, P. Bouyer, and M. A. Kasevich, Precision rotation measurements with an atom interferometer gyroscope, Phys. Rev. Lett. **78**, 2046 (1997).
[20] B. Canuel, F. Leduc, D. Holleville, A. Gauguet, J. Fils, A. Virdis, A. Clairon, N. Dimarcq, C. J. Bordé, A. Landragin, and P. Bouyer, Six-axis inertial sensor using cold-atom interferometry, Phys. Rev. Lett. **97**, 010402 (2006).
[21] Z.-X. Meng, P.-Q. Yan, S.-Z. Wang, X.-J. Li, H.-B. Xue, and Y.-Y. Feng, Closed-loop dual-atom-interferometer inertial sensor with continuous cold atomic beams, Phys. Rev. Appl. **21**, 034050 (2024).
[22] C. Salducci, Y. Bidel, M. Cadoret, S. Darmon, N. Za-

hzam, A. Bonnin, S. Schwartz, C. Blanchard, and A. Bresson, Quantum sensing of acceleration and rotation by interfering magnetically launched atoms, Science Advances **10**, eadq4498 (2024).
[23] A. Fregosi, C. Gabbanini, S. Gozzini, L. Lenci, C. Marinelli, and A. Fioretti, Magnetic induction imaging with a cold-atom radio frequency magnetometer, Appl. Phys. Lett. **117**, 144102 (2020).
[24] A. Fabricant, I. Novikova, and G. Bison, How to build a magnetometer with thermal atomic vapor: a tutorial, New Journal of Physics **25**, 025001 (2023).
[25] Z. Ma, C. Han, Z. Tan, H. He, S. Shi, X. Kang, J. Wu, J. Huang, B. Lu, and C. Lee, Adaptive cold-atom magnetometry mitigating the trade-off between sensitivity and dynamic range, Science Advances **11**, eadt3938 (2025).
[26] D. Boddice, N. Metje, and G. Tuckwell, Capability assessment and challenges for quantum technology gravity sensors for near surface terrestrial geophysical surveying, Journal of Applied Geophysics **146**, 149 (2017).
[27] N. Shettell, K. S. Lee, F. E. Oon, E. Maksimova, C. Hufnagel, S. Wei, and R. Dumke, Geophysical survey based on hybrid gravimetry using relative measurements and an atomic gravimeter as an absolute reference, Scientific Reports **14**, 6511 (2024).
[28] M. Diament, G. Lion, G. Pajot-Métivier, S. Merlet, and S. Déroussi, The AQG-B absolute quantum gravimeter: A promising sensor for volcano monitoring, IEEE Instrumentation & Measurement Magazine **27**, 17 (2024).
[29] M. J. Wright, L. Anastassiou, C. Mishra, J. M. Davies, A. M. Phillips, S. Maskell, and J. F. Ralph, Cold atom inertial sensors for navigation applications, Frontiers in Physics **10**, 994459 (2022).
[30] A. M. Phillips, M. J. Wright, M. Kiss-Toth, I. Read, I. Riou, S. Maddox, S. Maskell, and J. F. Ralph, Augmented inertial navigation using cold atom sensing, in *Cold Atoms for Quantum Technologies*, Vol. 11578, edited by S. Franke-Arnold, International Society for Optics and Photonics (SPIE, 2020) p. 115780C.
[31] E. Boto, N. Holmes, J. Legget, G. Roberts, V. Shah, S. Meyer, L. Munoz, K. Mullinger, T. Tierney, Bestmann, *et al.*, Moving magnetoencephalography towards real-world applications with a wearable system, Nature **555**, 657 (2018).
[32] T. M. Tierney, N. Holmes, S. Mellor, J. D. López, G. Roberts, R. M. Hill, E. Boto, J. Leggett, V. Shah, M. J. Brookes, R. Bowtell, and G. R. Barnes, Optically pumped magnetometers: From quantum origins to multi-channel magnetoencephalography, NeuroImage **199**, 598 (2019).
[33] Q.-Q. Guo, T. Hu, X.-Y. Feng, M.-K. Zhang, C.-Q. Chen, X. Zhang, Z.-K. Yao, J.-Y. Xu, Q. Wang, F.-Y. Fu, Y. Zhang, Y. Chang, and X.-D. Yang, A compact and closed-loop spin-exchange relaxation-free atomic magnetometer for wearable magnetoencephalography, Chinese Physics B **32**, 040702 (2023).
[34] B. Zhao, L. Li, Y. Zhang, J. Tang, Y. Liu, and Y. Zhai, Optically pumped magnetometers recent advances and applications in biomagnetism: A review, IEEE Sensors Journal **23**, 18949 (2023).
[35] H. Wang, M. Zugenmaier, K. Jensen, W. Zheng, and E. S. Polzik, Magnetic induction sensor based on a dual-frequency atomic magnetometer, Phys. Rev. Appl. **22**, 034030 (2024).
[36] Y. Bidel, O. Carraz, R. Charriere, M. Cadoret, N. Zahzam, and A. Bresson, Compact cold atom gravimeter for field applications, Appl. Phys. Lett. **102**, 144107 (2013).
[37] V. Menoret, P. Vermeulen, N. Le Moigne, S. Bonvalot, P. Bouyer, A. Landragin, and B. Desruelle, Gravity measurements below 10^{-9} g with a transportable absolute quantum gravimeter, Sci. Rep. **8**, 12300 (2018).
[38] C.-Y. Li, J.-B. Long, M.-Q. Huang, B. Chen, Y.-M. Yang, X. Jiang, C.-F. Xiang, Z.-L. Ma, D.-Q. He, L.-K. Chen, and S. Chen, Continuous gravity measurement with a portable atom gravimeter, Phys. Rev. A **108**, 032811 (2023).
[39] M. Limes, E. Foley, T. Kornack, S. Caliga, S. McBride, A. Braun, W. Lee, V. Lucivero, and M. Romalis, Portable magnetometry for detection of biomagnetism in ambient environments, Phys. Rev. Appl. **14**, 011002 (2020).
[40] Y. Zhao, D. Li, J. Niu, S. Bao, K. Zhang, Y. Wang, B. Cheng, C. Zhang, K. Niu, Y. Liu, Y. Yue, X. Wang, B. Wu, and Q. Lin, The implementation of a compact cold atom interference gyroscope based on miniaturized quartz vacuum chamber, IEEE Sensors Journal **24**, 40507 (2024).
[41] A. Belenchia, M. Carlesso, Ö. Bayraktar, D. Dequal, I. Derkach, G. Gasbarri, W. Herr, Y. L. Li, M. Rademacher, J. Sidhu, *et al.*, Quantum physics in space, Physics Reports **951**, 1 (2022).
[42] F. Migliaccio, M. Reguzzoni, K. Batsukh, G. M. Tino, G. Rosi, F. Sorrentino, C. Braitenberg, T. Pivetta, D. F. Barbolla, and S. Zoffoli, MOCASS: A satellite mission concept using cold atom interferometry for measuring the earth gravity field, Surveys in Geophysics **40**, 1029 (2019).
[43] R. Haagmans, C. Siemes, L. Massotti, O. Carraz, and P. Silvestrin, ESA's next-generation gravity mission concepts, Rendiconti Lincei. Scienze Fisiche e Naturali **31**, 15 (2020).
[44] M. He, X. Chen, J. Fang, Q. Chen, H. Sun, Y. Wang, J. Zhong, L. Zhou, C. He, J. Li, D. Zhang, G. Ge, W. Wang, Y. Zhou, X. Li, X. Zhang, L. Qin, Z. Chen, R. Xu, Y. Wang, Z. Xiong, J. Jiang, Z. Cai, K. Li, G. Zheng, W. Peng, J. Wang, and M. Zhan, The space cold atom interferometer for testing the equivalence principle in the china space station, npj Microgravity **9**, 58 (2023).
[45] F. Sorrentino, K. Bongs, P. Bouyer, L. Cacciapuoti, M. De Angelis, H. Dittus, W. Ertmer, A. Giorgini, J. Hartwig, M. Hauth, *et al.*, A compact atom interferometer for future space missions, Microgravity. Sci. Technol. **22**, 551 (2010).
[46] F. Müller, O. Carraz, P. Visser, and O. Witasse, Cold atom gravimetry for planetary missions, Planetary and Space Science **194**, 105110 (2020).
[47] L. Badurina, E. Bentine, D. Blas, K. Bongs, D. Bortoletto, T. Bowcock, K. Bridges, W. Bowden, O. Buchmueller, C. Burrage, *et al.*, AION: an atom interferometer observatory and network, J. Cosmol. Astropart. Phys. **2020**, 011 (2020).
[48] F. Wang, N. Cooper, Y. He, B. Hopton, D. Johnson, P. Zhao, C. J. Tuck, R. Hague, T. M. Fromhold, R. D. Wildman, *et al.*, Additive manufacturing of functionalised atomic vapour cells for next-generation

quantum technologies, Quantum Science and Technology **10**, 015019 (2024).
[49] S. Xu, X. Xia, Q. Yu, S. Khan, E. Megidish, B. You, B. Hemmerling, A. Jayich, J. Biener, and H. Häffner, 3D-printed micro ion trap technology for scalable quantum information processing, arXiv preprint arXiv:2310.00595 10.48550/arXiv.2310.00595 (2023).
[50] G. Kara, S. Bolat, K. Sharma, M. J. Grotevent, D. N. Dirin, D. Bachmann, R. Furrer, L. F. Boesel, Y. E. Romanyuk, R. M. Rossi, *et al.*, Conformal integration of an inkjet-printed PbS QDs-graphene IR photodetector on a polymer optical fiber, Advanced Materials Technologies **8**, 2201922 (2023).
[51] M. Christ, C. Zimmermann, S. Neinert, B. Leykauf, K. Döringshoff, and M. Krutzik, Additively manufactured ceramics for compact quantum technologies, Advanced Quantum Technologies **7**, 2400076 (2024).
[52] S. Madkhaly, L. Coles, C. Morley, C. Colquhoun, M. Fromhold, N. Cooper, and L. Hackermüller, Performance-optimized components for quantum technologies via additive manufacturing, PRX Quantum **2**, 030326 (2021).
[53] R. M. Hill, E. Boto, M. Rea, N. Holmes, J. Leggett, L. A. Coles, M. Papastavrou, S. K. Everton, B. A. Hunt, D. Sims, J. Osborne, V. Shah, R. Bowtell, and M. J. Brookes, Multi-channel whole-head OPM-MEG: Helmet design and a comparison with a conventional system, NeuroImage **219**, 116995 (2020).
[54] F. Wang, N. Cooper, Y. He, B. Hopton, D. Johnson, P. Zhao, C. J. Tuck, R. Hague, T. M. Fromhold, R. D. Wildman, L. Turyanska, and L. Hackermüller, Additive manufacturing of functionalised atomic vapour cells for next-generation quantum technologies, Quantum Science and Technology **10**, 015019 (2024).
[55] H. Stærkind, K. Jensen, J. H. Müller, V. O. Boer, E. T. Petersen, and E. S. Polzik, Precision measurement of the excited state landé g-factor and diamagnetic shift of the cesium D_2 line, Phys. Rev. X **13**, 021036 (2023).
[56] A. Sigel, M. Merkel, and A. Heinrich, Miniaturization of an optical 3D sensor by additive manufacture of metallic mirrors, in *Optical Measurement Systems for Industrial Inspection X*, Vol. 10329 (SPIE, 2017) pp. 165–176.
[57] J. Vovrosh, G. Voulazeris, P. G. Petrov, J. Zou, Y. Gaber, L. Benn, D. Woolger, M. M. Attallah, V. Boyer, K. Bongs, and M. Holynski, Additive manufacturing of magnetic shielding and ultra-high vacuum flange for cold atom sensors, Scientific Reports **8**, 2023 (2018).
[58] R. Saint, W. Evans, Y. Zhou, T. Barrett, T. M. Fromhold, E. Saleh, I. Maskery, C. Tuck, R. Wildman, F. Oručević, and P. Krüger, 3D-printed components for quantum devices, Scientific Reports **8**, 8368 (2018).
[59] M. Shusteff, A. E. Browar, B. E. Kelly, J. Henriksson, T. H. Weisgraber, R. M. Panas, N. X. Fang, and C. M. Spadaccini, One-step volumetric additive manufacturing of complex polymer structures, Science Advances **3**, eaao5496 (2017).
[60] M. Carlotti and V. Mattoli, Functional materials for two-photon polymerization in microfabrication, Small **15**, 1902687 (2019).
[61] D. E. Marschner, S. Pagliano, P.-H. Huang, and F. Niklaus, A methodology for two-photon polymerization micro 3D printing of objects with long overhanging structures, Additive Manufacturing **66**, 103474 (2023).
[62] J. Im, Y. Liu, Q. Hu, G. F. Trindade, C. Parmenter, M. Fay, Y. He, D. J. Irvine, C. Tuck, R. D. Wildman, *et al.*, Strategies for integrating metal nanoparticles with two-photon polymerization process: Toward high resolution functional additive manufacturing, Advanced Functional Materials **33**, 2211920 (2023).
[63] F. Kotz, K. Arnold, W. Bauer, D. Schild, N. Keller, K. Sachsenheimer, T. M. Nargang, C. Richter, D. Helmer, and B. E. Rapp, Three-dimensional printing of transparent fused silica glass, Nature **544**, 337 (2017).
[64] O. Nelson-Dummett, G. Rivers, N. Gilani, M. Simonelli, C. J. Tuck, R. D. Wildman, R. J. Hague, and L. Turyanska, Off the grid: A new strategy for material-jet 3D printing with enhanced sub-droplet resolution, Additive Manufacturing Letters **8**, 100185 (2024).
[65] A. Bastola, Y. He, J. Im, G. Rivers, F. Wang, R. Worsley, J. S. Austin, O. Nelson-Dummett, R. D. Wildman, R. Hague, *et al.*, Formulation of functional materials for inkjet printing: A pathway towards fully 3D printed electronics, Materials Today Electronics , 100058 (2023).
[66] T. Carey, S. Cacovich, G. Divitini, J. Ren, A. Mansouri, J. M. Kim, C. Wang, C. Ducati, R. Sordan, and F. Torrisi, Fully inkjet-printed two-dimensional material field-effect heterojunctions for wearable and textile electronics, Nature communications **8**, 1202 (2017).
[67] B. W. An, K. Kim, H. Lee, S.-Y. Kim, Y. Shim, D.-Y. Lee, J. Y. Song, and J.-U. Park, High-resolution printing of 3D structures using an electrohydrodynamic inkjet with multiple functional inks, Advanced materials **27**, 4322 (2015).
[68] P. Yang, L. Zhang, D. J. Kang, R. Strahl, and T. Kraus, High-resolution inkjet printing of quantum dot light-emitting microdiode arrays, Advanced Optical Materials **8**, 1901429 (2020).
[69] J. S. Austin, N. D. Cottam, C. Zhang, F. Wang, J. H. Gosling, O. Nelson-Dummet, T. S. James, P. H. Beton, G. F. Trindade, Y. Zhou, *et al.*, Photosensitisation of inkjet printed graphene with stable all-inorganic perovskite nanocrystals, Nanoscale **15**, 2134 (2023).
[70] N. Cooper, L. Coles, S. Everton, I. Maskery, R. Campion, S. Madkhaly, C. Morley, J. O'shea, W. Evans, R. Saint, *et al.*, Additively manufactured ultra-high vacuum chamber for portable quantum technologies, Additive Manufacturing **40**, 101898 (2021).
[71] Y. Tang, G. Dong, Q. Zhou, and Y. F. Zhao, Lattice structure design and optimization with additive manufacturing constraints, IEEE Transactions on Automation Science and Engineering **15**, 1546 (2018).
[72] I. Maskery, A. Aremu, L. Parry, R. Wildman, C. Tuck, and I. Ashcroft, Effective design and simulation of surface-based lattice structures featuring volume fraction and cell type grading, Materials & Design **155**, 220 (2018).
[73] K. Clements, B. Elder, L. Hackermueller, M. Fromhold, and C. Burrage, Detecting dark domain walls through their impact on particle trajectories in tailored ultrahigh vacuum environments, Phys. Rev. D **109**, 123023 (2024).
[74] Y.-S. Leung, T.-H. Kwok, X. Li, Y. Yang, C. C. L. Wang, and Y. Chen, Challenges and status on design and computation for emerging additive manufacturing

technologies, Journal of Computing and Information Science in Engineering **19**, 021013 (2019).
[75] P. Vogiatzis, M. Ma, S. Chen, and X. D. Gu, Computational design and additive manufacturing of periodic conformal metasurfaces by synthesizing topology optimization with conformal mapping, Computer Methods in Applied Mechanics and Engineering **328**, 477 (2018).
[76] M. Bayat, O. Zinovieva, F. Ferrari, C. Ayas, M. Langelaar, J. Spangenberg, R. Salajeghe, K. Poulios, S. Mohanty, O. Sigmund, and J. Hattel, Holistic computational design within additive manufacturing through topology optimization combined with multiphysics multiscale materials and process modelling, Progress in Materials Science **138**, 101129 (2023).
[77] Y. Zhai, D. A. Lados, and J. L. LaGoy, Additive manufacturing: Making imagination the major limitation, JOM **66**, 808 (2014).
[78] M. E. Orme, M. Gschweitl, M. Ferrari, I. Madera, and F. Mouriaux, Designing for additive manufacturing: Lightweighting through topology optimization enables lunar spacecraft, Journal of Mechanical Design **139**, 100905 (2017).
[79] L. Chougrani, J.-P. Pernot, P. Véron, and S. Abed, Parts internal structure definition using non-uniform patterned lattice optimization for mass reduction in additive manufacturing, Engineering with Computers **35**, 277 (2019).
[80] S. Junk, B. Klerch, and U. Hochberg, Structural optimization in lightweight design for additive manufacturing, Procedia CIRP **84**, 277 (2019), 29th CIRP Design Conference 2019, 08-10 May 2019, Póvoa de Varzim, Portgal.
[81] K. V. Fetisov and P. V. Maksimov, Topology optimization and laser additive manufacturing in design process of efficiency lightweight aerospace parts, Journal of Physics: Conference Series **1015**, 052006 (2018).
[82] B. M. Nafis, R. Whitt, A.-C. Iradukunda, and D. Huitink, Additive manufacturing for enhancing thermal dissipation in heat sink implementation: A review, Heat Transfer Engineering **42**, 967 (2021).
[83] G. Favero, M. Bonesso, P. Rebesan, R. Dima, A. Pepato, and S. Mancin, Additive manufacturing for thermal management applications: from experimental results to numerical modeling, International Journal of Thermofluids **10**, 100091 (2021).
[84] W. Elmadih, *Additively manufactured lattice structures for vibration attenuation*, Ph.D. thesis, University of Nottingham (2020).
[85] F. Xue, H. Boudaoud, G. Robin, F. A. C. Sanchez, and E. M. Daya, Enhancing vibration damping properties of additively manufactured viscoelastic structures through process parameter optimization, Mechanics of Advanced Materials and Structures **31**, 7515 (2024).
[86] D. Mayer, H. A. Stoffregen, O. Heuss, J. Thiel, E. Abele, and T. Melz, Additive manufacturing of active struts for piezoelectric shunt damping, Journal of Intelligent Material Systems and Structures **27**, 743 (2016).
[87] S. Madkhaly, N. Cooper, L. Coles, and L. Hackermüller, High-performance, additively-manufactured atomic spectroscopy apparatus for portable quantum technologies, Opt. Express. **30**, 25753 (2022).
[88] M. Christ, O. Anton, C. Zimmermann, V. A. Henderson, E. D. Ros, and M. Krutzik, Micro-integrated crossed-beam optical dipole trap system with long-term alignment stability for mobile atomic quantum technologies, Opt. Express **32**, 40806 (2024).
[89] S. Jenzer, M. Alves, N. Delerue, A. Gonnin, D. Grasset, F. Letellier-Cohen, B. Mercier, E. Mistretta, C. Prevost, A. Vion, and J.-P. Wilmes, Study of the suitability of 3D printing for ultra-high vacuum applications, Journal of Physics: Conference Series **874**, 012097 (2017).
[90] J. Lee, R. Ding, J. Christensen, R. R. Rosenthal, A. Ison, D. P. Gillund, D. Bossert, K. H. Fuerschbach, W. Kindel, P. S. Finnegan, J. R. Wendt, M. Gehl, A. Kodigala, H. McGuinness, C. A. Walker, S. A. Kemme, A. Lentine, G. Biedermann, and P. D. D. Schwindt, A compact cold-atom interferometer with a high data-rate grating magneto-optical trap and a photonic-integrated-circuit-compatible laser system, Nature Communications **13**, 5131 (2022).
[91] E. B. Norrgard, D. S. Barker, J. A. Fedchak, N. Klimov, J. Scherschligt, and S. Eckel, Note: A 3D-printed alkali metal dispenser, Review of Scientific Instruments **89**, 056101 (2018).
[92] S. Jenzer, M. Alves, S. Bilgen, J. Bonis, F. Brisset, S. Djelali, A. Gonnin, M. Guerrier, D. Grasset, F. Letellier-Cohen, B. Mercier, E. Mistretta, and G. Sattonnay, Is it possible to use additive manufacturing for accelerator uhv beam pipes?, Journal of Physics: Conference Series **1350**, 012199 (2019).
[93] A. Ratkus, S. Rarison, C. Garion, H. Kos, S. Gruber, L. Stepien, A. A. Patil, E. Lopez, T. Torims, G. Pikurs, M. Vedani, and V. Lacis, Evaluation of green laser source additive manufacturing technology for accelerator applications with ultra-high vacuum requirements, Journal of Physics: Conference Series **2687**, 082046 (2024).
[94] M. Ziaee and N. B. Crane, Binder jetting: A review of process, materials, and methods, Additive Manufacturing **28**, 781 (2019).
[95] A. Domingues, A. Martínez-Carboneres, and S. Carlson, Evaluation of 3D-printed plastics for ultra-high vacuum applications: Outgassing, and residual gas analysis, Vacuum **233**, 113970 (2025).
[96] J. Li, T. Mcpartland, B. Gutierrez, J. Pedersen, and Y. Zhou, Additive manufacturing for ultra-high vacuum components: Leveraging photo-polymer resin technologies, Vacuum **220**, 112769 (2024).
[97] I. T. Heikkinen, G. Marin, N. Bihari, C. Ekstrum, P. J. Mayville, Y. Fei, Y. H. Hu, M. Karppinen, H. Savin, and J. M. Pearce, Atomic layer deposited aluminum oxide mitigates outgassing from fused filament fabrication–based 3-D printed components, Surface and Coatings Technology **386**, 125459 (2020).
[98] N. Cooper, D. Johnson, B. Hopton, M. Overton, L. Hackermüller, D. Stupple, A. Bratu, E. Wilson, J. Robinson, L. Coles, and M. Papastavrou, 3D-printed surfaces enhance passive pumping for portable quantum technologies, Manuscript in preparation.
[99] D. Xie, H. Zhang, X. Shu, and J. Xiao, Fabrication of polymer micro-lens array with pneumatically diaphragm-driven drop-on-demand inkjet technology, Optics Express **20**, 15186 (2012).
[100] R. Guo, S. Xiao, X. Zhai, J. Li, A. Xia, and W. Huang, Micro lens fabrication by means of femtosecond two photon photopolymerization, Optics Express **14**, 810 (2006).
[101] M. Sartison, S. L. Portalupi, T. Gissibl, M. Jetter,

H. Giessen, and P. Michler, Combining in-situ lithography with 3D printed solid immersion lenses for single quantum dot spectroscopy, Scientific Reports **7**, 39916 (2017).

[102] F. A. Couto, M. B. Andrade, A. J. Otuka, S. Pratavieira, S. R. Muniz, and C. R. Mendonça, Integrating fluorescent nanodiamonds into polymeric microstructures fabricated by two-photon polymerization, Nanomaterials **13**, 2571 (2023).

[103] D. J. Lorang, D. Tanaka, C. M. Spadaccini, K. A. Rose, N. J. Cherepy, and J. A. Lewis, Photocurable liquid core–fugitive shell printing of optical waveguides, Advanced Materials **23**, 5055 (2011).

[104] J. Pyo, J. Kim, J. Lee, J. Yoo, and J. H. Je, 3D printed nanophotonic waveguides, Adv. Optical Mater. **4**, 1190 (2016).

[105] M. Sartison, K. Weber, S. Thiele, L. Bremer, S. Fischbach, T. Herzog, S. Kolatschek, M. Jetter, S. Reitzenstein, A. Herkommer, P. Michler, S. L. Portalupi, and H. Giessen, 3D printed micro-optics for quantum technology: Optimised coupling of single quantum dot emission into a single-mode fibre, Light: Advanced Manufacturing **2**, 103 (2021).

[106] V. Dragone, V. Sans, M. H. Rosnes, P. J. Kitson, and L. Cronin, 3D-printed devices for continuous-flow organic chemistry, Beilstein Journal of Organic Chemistry **9**, 951 (2013).

[107] B. T. Flinn, V. Radu, M. W. Fay, A. J. Tyler, J. Pitcairn, M. J. Cliffe, B. L. Weare, C. T. Stoppiello, M. L. Mather, and A. N. Khlobystov, Nitrogen vacancy defects in single-particle nanodiamonds sense paramagnetic transition metal spin noise from nanoparticles on a transmission electron microscopy grid, Nanoscale Advances **5**, 6423 (2023).

[108] V. Radu, J. C. Price, S. J. Levett, K. K. Narayanasamy, T. D. Bateman-Price, P. B. Wilson, and M. L. Mather, Dynamic quantum sensing of paramagnetic species using nitrogen-vacancy centers in diamond, ACS Sensors **5**, 703 (2019).

[109] U. Mangal, J.-Y. Seo, J. Yu, J.-S. Kwon, and S.-H. Choi, Incorporating aminated nanodiamonds to improve the mechanical properties of 3D-printed resin-based biomedical appliances, Nanomaterials **10**, 827 (2020).

[110] E. Da Ros, N. Cooper, J. Nute, and L. Hackermueller, Cold atoms in micromachined waveguides: A new platform for atom-photon interactions, Phys. Rev. Res. **2**, 033098 (2020).

[111] J. B. Spring, B. J. Metcalf, P. C. Humphreys, W. S. Kolthammer, X.-M. Jin, M. Barbieri, A. Datta, N. Thomas-Peter, N. K. Langford, D. Kundys, J. C. Gates, B. J. Smith, P. G. R. Smith, and I. A. Walmsley, Boson sampling on a photonic chip, Science **339**, 798 (2013).

[112] N. Cooper, E. Da Ros, C. Briddon, V. Naniyil, M. T. Greenaway, and L. Hackermueller, Prospects for strongly coupled atom-photon quantum nodes, Scientific Reports **9**, 7798 (2019).

[113] T. Gissibl, S. Thiele, A. Herkommer, and H. Giessen, Sub-micrometre accurate free-form optics by three-dimensional printing on single-mode fibres, Nature Communications **7**, 11763 (2016).

[114] P. Ruchka, S. Hammer, M. Rockenhäuser, R. Albrecht, J. Drozella, S. Thiele, H. Giessen, and T. Langen, Microscopic 3D printed optical tweezers for atomic quantum technology, Quantum Science and Technology **7**, 045011 (2022).

[115] B. Derby, Inkjet printing of functional and structural materials: fluid property requirements, feature stability, and resolution, Annual Review of Materials Research **40**, 395 (2010).

[116] S. C. Jensen, J. D. Carroll, P. R. Pathare, D. J. Saiz, J. W. Pegues, B. L. Boyce, B. H. Jared, and M. J. Heiden, Long-term process stability in additive manufacturing, Additive Manufacturing **61**, 103284 (2023).

[117] A. D. Valentine, T. A. Busbee, J. W. Boley, J. R. Raney, A. Chortos, A. Kotikian, J. D. Berrigan, M. F. Durstock, and J. A. Lewis, Hybrid 3D printing of soft electronics, Advanced Materials **29**, 1703817 (2017).

[118] A. A. Krimpenis and G. D. Noeas, Application of hybrid manufacturing processes in microfabrication, Journal of Manufacturing Processes **80**, 328 (2022).